Exchange-Correlation Energy from Pairing Matrix Fluctuation and the Particle-Particle Random Phase Approximation

Helen van Aggelen

Ghent University, Department of Inorganic and Physical Chemistry, Ghent, Belgium and

Duke University, Department of Chemistry, Durham, NC 27708, U.S.

Yang Yang

Duke University, Department of Chemistry, Durham, NC 27708, U.S.

Weitao Yang

Duke University, Department of Chemistry and

Department of Physics, Durham, NC 27708, U.S.

(Dated: January 30, 2014)

Abstract

Despite their unmatched success for many applications, commonly used local, semi-local and hybrid density functionals still face challenges when it comes to describing long-range interactions, static correlation and electron delocalization. Density functionals of both the occupied and virtual orbitals are able to address these problems. The particle-hole (ph-) Random Phase Approximation (RPA), a functional of occupied and virtual orbitals, has recently known a revival within the DFT community.

Following up on an idea introduced in our recent communication [PRA 88, 030501 (2013)], we formulate more general adiabatic connections for the correlation energy in terms of pairing matrix fluctuations described by the particle-particle (pp-) propagator. With numerical examples of the pp-RPA, the lowest-order approximation to the pp-propagator, we illustrate the potential of density functional approximations based on pairing matrix fluctuations. The pp-RPA is size-extensive, self-interaction free, fully anti-symmetric, describes the strong static correlation limit in H_2 and eliminates delocalization errors in H_2^+ and other single-bond systems. It gives surprisingly good non-bonded interaction energies – competitive with the ph-RPA – with the correct R^{-6} asymptotic decay as a function of the separation R, which we argue is mainly attributable to its correct second-order energy term. While the pp-RPA tends to underestimate absolute correlation energies, it gives good relative energies: much better atomization energies than the ph-RPA, as it has no tendency to underbind, and reaction energies of similar quality. The adiabatic connection in terms of pairing matrix fluctuation paves the way for promising new density functional approximations.

I. INTRODUCTION

Density functional approximations based on many-body perturbation techniques may offer solutions to some of the challenges density functional approximations continue to face. Commonly used local, semi-local generalized gradient and hybrid density functional approximations (DFA's) are unmatched in their success for many applications, but are unable to deal with several fundamental problems for which there is no straightforward solution [1]. The most prominent problems, such as their persistent delocalization and static correlation errors and inability to capture long-range interactions, are extremely difficult to solve within the simple framework of (semi-)local smooth functionals of the density or gradient [2–4]. Continuous functionals of the density or the Kohn-Sham density matrix are incapable of describing the discontinuous piecewise-linear nature of the exact energy functional[5], which lies at the heart of the static correlation and delocalization errors observed in density functional approximations [4, 6]. Local and semi-local functionals are unable to describe long-range interactions, which require a fully non-local functional [7, 8]. As a consequence, slightly more complex ab initio methods that can still be formulated in a computationally efficient manner provide attractive alternatives as computer speeds continue to increase [9–12]. The most notable density functional method of this kind is perhaps the particle-hole Random Phase Approximation (ph-RPA) [12, 13]. The ph-RPA can be viewed as a density functional through the adiabatic connection [14, 15] and fluctuation-dissipation[16] (ACFD) theorem. The adiabatic connection forms a direct link between the correlation energy in the DFT perspective and the polarization propagator, which describes density fluctuations in many-body perturbation theory. The ph-RPA provides an approximation to the polarization propagator and leads to a simple analytical expression for the correlation energy, equivalent to the sum of all ring diagrams[17, 18] (in this context, the ph-RPA is almost exclusively used in its 'direct' formulation, which neglects the exchange terms in the two-electron integrals, and so we will use to term 'ph-RPA' to denote the direct ph-RPA). Efficient implementations reduce its computational cost to $O(M^4)$ [19, 20], $O(M^3)$[21] or even $O(M^2)$[22] with M a measure of the system size – competitive with the cost of a Hartree-Fock calculation. The ph-RPA has several merits compared to commonly used DFA's: it is fully non-local, describes long-range interactions [7, 23–25], eliminates static correlation errors (it gives the correct dissociation limit for H_2, for instance [26]) and is applicable to systems with vanishing

gap. But it has large delocalization errors [27].

Following an idea introduced in a recent communication[28], we formulate an alternative adiabatic connection for the correlation energy in terms of the particle-particle propagator, or, equivalently, the pairing matrix fluctuation, set forth in section II. The adiabatic connection we formulate is similar in form to the well-known ACFD theorem. It is in principle exact. It thus provides a basis for developing density functional approximations based on pairing matrix fluctuations. The most straightforward approximation is the pp-RPA [17, 29], the lowest-order approximation to the pp-propagator. As section II illustrates, it is similar in form to the ph-RPA. The pp-RPA is a well-known technique to describe nuclear many-body effects [29], but in contrast to the ph-RPA it has not received much attention within the DFT community. Like the ph-RPA, the pp-RPA can be viewed as an alternative formulation of a coupled-cluster method: the pp-RPA correlation energy amounts to the sum of all ladder diagrams [17]. As such, it is equivalent to coupled-cluster doubles (CCD) restricted to ladder diagrams [30–32]. Although the adiabatic connection we formulate lays the foundations for a wealth of approximations based on pairing matrix fluctuations, we will take the pp-RPA to be a representative of density functional approximations based on pairing matrix fluctuations and the ph-RPA as a representative of functionals based on density fluctuations. Section IV illustrates some of the main differences between the two types of RPA with numerical examples.

II. PAIRING MATRIX FLUCTUATIONS AND THE ADIABATIC CONNECTION

A. Pairing matrix fluctuations

The particle-particle propagator describes instantaneous pairing matrix fluctuations. For a system with a fixed number of electrons N, for which $\langle \hat{N}^2 \rangle = \langle \hat{N} \rangle^2$, the pairing matrix κ is identically zero, because it involves components of the wavefunction with different electron number,

$$\kappa_{ij} = \langle \Psi_0 | a_i a_j | \Psi_0 \rangle.$$

Although most quantum chemical methods restrict themselves to eigenstates of the electron number operator $\hat{N}$, it may be beneficial to break particle number symmetry while preserving

the electron number expectation value, $\langle \hat{N} \rangle = N$ [10]. In its time-dependent form, the retarded particle-particle (pp-) propagator,

$$\bar{K}_{ijkl}(t-t') = \frac{-i}{\hbar}\theta(t-t')\langle \Psi_0^N | [a_{H_i}(t)a_{H_j}(t), a^\dagger_{H_l}(t')a^\dagger_{H_k}(t')] | \Psi_0^N \rangle, \tag{1}$$

describes the response of the pairing matrix to a perturbation in the form of a pairing field, $\hat{F}(t) = \sum_{kl} f_{kl}(t) a_l^\dagger a_k^\dagger \theta(t)$. The operators $a^\dagger_{H_i}(t)$ are the creation operators in the Heisenberg picture, $a^\dagger_{H_i}(t) = e^{\frac{i}{\hbar}(\hat{H}-\nu\hat{N})} a_i^\dagger e^{\frac{-i}{\hbar}(\hat{H}-\nu\hat{N})}$ and the term $-\nu\hat{N}$, with ν the chemical potential, is added to the Hamiltonian such that the N-electron state is the minimum under the total Hamiltonian $\hat{H} - \nu\hat{N}$ when the particle number is allowed to change. Under the influence of such a pairing perturbation, the pairing matrix no longer vanishes, and its change is described by the pp-propagator in the linear response regime:

$$\begin{aligned}
\kappa_{ij}(t) &= \frac{-i}{\hbar}\int_{-\infty}^{+\infty} \langle \Psi_0^N | [a_{H_i}(t)a_{H_j}(t), \hat{F}_H(t')] | \Psi_0^N \rangle dt' \\
&= \int_{-\infty}^{+\infty} \sum_{kl} \bar{K}(t-t')_{ijkl} f_{kl}(t') dt'
\end{aligned}$$

where $\hat{F}_H(t) = \sum_{kl} f_{kl} a^\dagger_{H_l}(t) a^\dagger_{H_k}(t)\theta(t)$ is the Heisenberg form of the pairing field. Since the pairing matrix vanishes for the N-electron ground state, the particle-particle propagator completely describes the dynamic fluctuation of the pairing matrix, i.e.

$$\bar{K}_{ijkl}(t-t') = \frac{-i}{\hbar}\theta(t-t')\langle \Psi_0^N | [\left(a_{H_i}(t)a_{H_j}(t) - \langle a_i a_j \rangle\right), \left(a^\dagger_{H_l}(t')a^\dagger_{H_k}(t') - \langle a_l^\dagger a_k^\dagger \rangle\right)] | \Psi_0^N \rangle.$$

From its Fourier transform to the energy domain it is apparent that the retarded particle-particle propagator characterizes double electron addition and ionization processes,

$$\begin{aligned}
\bar{K}(E)_{ijkl} &= \int_{-\infty}^{+\infty} e^{\frac{i}{\hbar}E(t-t')} \bar{K}_{ijkl}(t-t') d(t-t') \\
&= \sum_n \frac{\langle \Psi_0^N | a_i a_j | \Psi_n^{N+2} \rangle \langle \Psi_n^{N+2} | a_l^\dagger a_k^\dagger | \Psi_0^N \rangle}{E - \omega_n^{N+2} + i\eta} \\
&\quad - \sum_n \frac{\langle \Psi_0^N | a_l^\dagger a_k^\dagger | \Psi_n^{N-2} \rangle \langle \Psi_n^{N-2} | a_i a_j | \Psi_0^N \rangle}{E - \omega_n^{N-2} + i\eta},
\end{aligned} \tag{2}$$

since its poles determine the double electron addition and ionization energies, $\omega_n^{N+2} = E_n^{N+2} - E_0^N - 2\nu$ and $\omega_n^{N-2} = E_0^N - E_n^{N-2} - 2\nu$, and the residues determine the corresponding transition amplitudes. These properties of the pp-propagator have been used to compute Auger spectra, which involve double ionization processes, with the pp-RPA [33, 34].

The time-ordered pp-propagator $\mathbf{K}$,

$$K_{ijkl}(t-t') = \frac{-i}{\hbar}\langle\Psi_0^N|\mathcal{T}[a_{H_i}(t)a_{H_j}(t)a_{H_l}^\dagger(t')a_{H_k}^\dagger(t')]|\Psi_0^N\rangle$$

with $\mathcal{T}$ the time-ordering operator, differs only from the retarded propagator $\bar{\mathbf{K}}$ in the position of its poles in the negative real plane,

$$\begin{aligned} K_{ijkl}(E) &= \int_{-\infty}^{+\infty} e^{\frac{i}{\hbar}E(t-t')}K_{ijkl}(t-t')d(t-t') \\ &= \sum_n \frac{\langle\Psi_0^N|a_i a_j|\Psi_n^{N+2}\rangle\langle\Psi_n^{N+2}|a_l^\dagger a_k^\dagger|\Psi_0^N\rangle}{E-\omega_n^{N+2}+i\eta} \\ &\quad - \sum_n \frac{\langle\Psi_0^N|a_l^\dagger a_k^\dagger|\Psi_n^{N-2}\rangle\langle\Psi_n^{N-2}|a_i a_j|\Psi_0^N\rangle}{E-\omega_n^{N-2}-i\eta}. \end{aligned} \tag{3}$$

The retarded and time-ordered propagator therefore carry much of the same physical information. However, as is the case with the linear response, it is often more convenient to adopt the time-ordered propagator to which the methodology of many-body perturbation theory applies [35].

For a non-interacting reference wavefunction, the particle-particle propagator $\mathbf{K}^0$ becomes

$$\begin{aligned} K_{ijkl}^0(E) &= \delta_{ik}\delta_{jl}\frac{\theta(i-F)\theta(j-F)}{E-(\epsilon_i+\epsilon_j-2\nu)+i\eta} \\ &\quad - \delta_{ik}\delta_{jl}\frac{\theta(F-i)\theta(F-j)}{E-(\epsilon_i+\epsilon_j-2\nu)-i\eta} \end{aligned} \tag{4}$$

where F denotes the Fermi level and θ the Heaviside function, so the left term generates particle-particle terms and the right term generates hole-hole terms. As the pp-propagator is antisymmetric under the exchange of two electrons, $K_{ijkl}(E) = -K_{jikl}(E)$, we have used here (and in the following) an antisymmetric basis in which the two-particle indices ij are restricted, $i < j$. The non-interacting propagator is the particle-particle propagator in the uncorrelated limit, and provides a basis in which the exact propagator is approximated in many-body perturbation theory. The adiabatic connection is particularly valuable in this context, as it forms an energetic link between the the exact, fully interacting, system described by $\mathbf{K}$ and the non-interacting reference system described by $\mathbf{K}^0$.

B. Adiabatic connections in terms of pairing matrix fluctuations

The pp-propagator describes pairing matrix fluctuations and, similar to the well-known ACFD theorem, pairing matrix fluctuations determine the correlation energy via the adia-

batic connection. We formulate such an adiabatic connection in this section. It relates the linear response of a system under an external pairing perturbation to its correlation energy in equilibrium and is therefore also a type of fluctuation-dissipation theorem[16].

The energy of a system involving at most two-particle interactions is determined by its second order density matrix Γ,

$$\begin{aligned}\Gamma_{ijkl} &= \langle\Psi_0^N|a_i^\dagger a_j^\dagger a_l a_k|\Psi_0^N\rangle \\ &= \sum_n \langle\Psi_0^N|a_i^\dagger a_j^\dagger|\Psi_n^{N-2}\rangle\langle\Psi_n^{N-2}|a_l a_k|\Psi_0^N\rangle, \end{aligned} \tag{5}$$

but it can also be formulated in terms of other second-order metric matrices, like the G-matrix G,

$$\begin{aligned}G_{ijkl} &= \langle\Psi_0^N|a_i^\dagger a_j a_l^\dagger a_k|\Psi_0^N\rangle \\ &= \sum_n \langle\Psi_0^N|a_i^\dagger a_j|\Psi_n^N\rangle\langle\Psi_n^N|a_l^\dagger a_k|\Psi_0^N\rangle, \end{aligned} \tag{6}$$

In the second line in Eqs. (5) and (6) we have used the completeness of the basis to make the relationship between these second-order metric matrices and the residues of the propagators (such as Eq.(3)) more apparent. All such second-order metric matrices are linearly interrelated via the anti-commutation relationships of the creation and annihilation operators; for instance $\Gamma_{ijkl} = -G_{ilkj} + \delta_{jl}\gamma_{ik} = G_{jlki} - \delta_{il}\gamma_{jk}$, where γ_{ik} is the first-order density matrix, $\gamma_{ij} = \langle\Psi_0^N|a_i^\dagger a_j|\Psi_0^N\rangle$. As a consequence, the adiabatic connection can be formulated equivalently in terms of G and Γ. The adiabatic connection path is defined by the Hamiltonian $\hat{H}_\lambda$

$$\hat{H}_\lambda = \hat{h} + \hat{u}_\lambda + \lambda\hat{V} \tag{7}$$

where $\hat{h} = \hat{t} + \hat{v}_{ext}$ and $\hat{u}_\lambda$ is so far only specified in the limits $\lambda = 0$ and $\lambda = 1$: $\hat{u}_0$ is the effective potential that defines the non-interacting reference system and $\hat{u}_1 = 0$. This ensures that $\hat{H}_\lambda$ corresponds to the non-interacting Hamiltonian $\hat{H}_0$ when $\lambda = 0$ and to the physical Hamiltonian $\hat{H}$ when $\lambda = 1$. The adiabatic connection is then

$$\begin{aligned}E - E^0 &= \int_0^1 \langle\Psi^\lambda|\frac{\partial\hat{H}_\lambda}{\partial\lambda}|\Psi^\lambda\rangle d\lambda \\ &= \mathrm{tr}\int_0^1 \mathbf{V}\mathbf{\Gamma}^\lambda d\lambda + \mathrm{tr}\int_0^1 \frac{\partial\mathbf{u}_\lambda}{\partial\lambda}\gamma^\lambda d\lambda,\end{aligned}$$

where

$$E^0 = \langle \Psi^0 | \hat{H}_0 | \Psi^0 \rangle$$
$$= \text{tr } (\mathbf{h} + \mathbf{u}_0)\gamma^0.$$

Using the exact exchange functional,

$$E^{HF}[\gamma^0] = \langle \Psi^0 | \hat{H} | \Psi^0 \rangle$$
$$= \text{tr } \int_0^1 \mathbf{V}\mathbf{\Gamma}^0 d\lambda + \text{tr } \hat{h}\gamma^0,$$

as a reference, the correlation energy $E^c \equiv E - E^{HF}[\gamma^0]$ becomes

$$E^c = \text{tr } \int_0^1 \mathbf{V}(\mathbf{\Gamma}^\lambda - \mathbf{\Gamma}^0) d\lambda + \text{tr } \mathbf{u}_0\gamma^0$$
$$+ \text{tr } \int_0^1 \frac{\partial \mathbf{u}_\lambda}{\partial \lambda}\gamma^\lambda d\lambda.$$

Given the linear relation between the second order density matrix and the G-matrix, this gives rise to two equivalent formulae for the correlation energy:

$$E^c = \text{tr } \int_0^1 \mathbf{V}(\mathbf{\Gamma}^\lambda - \mathbf{\Gamma}^0) d\lambda + \text{tr } \mathbf{u}_0\gamma^0 + \text{tr } \int_0^1 \frac{\partial \mathbf{u}_\lambda}{\partial \lambda}\gamma^\lambda d\lambda \tag{8}$$

$$E^c = \text{tr } \int_0^1 \tilde{\mathbf{V}}(\mathbf{G}^\lambda - \mathbf{G}^0) d\lambda - \sum_{ijk} \int_0^1 \langle ij|ki\rangle (\gamma^\lambda_{jk} - \gamma^0_{jk}) d\lambda$$
$$+ \text{tr } \mathbf{u}_0\gamma^0 + \text{tr } \int_0^1 \frac{\partial \mathbf{u}_\lambda}{\partial \lambda}\gamma^\lambda d\lambda, \tag{9}$$

where

$$\langle ij|kl\rangle = \int \frac{\phi_i^*(\mathbf{x}_1)\phi_j^*(\mathbf{x}_2)\phi_k(\mathbf{x}_1)\phi_l(\mathbf{x}_2)}{|\mathbf{r}_1 - \mathbf{r}_2|} d\mathbf{x}_1 d\mathbf{x}_2,$$

$\tilde{V}_{ijkl} = \langle il|jk\rangle$ and $V_{ijkl} = \langle ij||kl\rangle = \langle ij|kl\rangle - \langle ji|kl\rangle$. There are several ways to choose the adiabatic connection path. Conventionally, the ph-RPA has been used in conjunction with the constant-density adiabatic connection path [14]. In the following paragraphs, we formulate the constant-density adiabatic connection path in terms of pairing matrix fluctuations and explore more general integration schemes.

1. *Constant-density adiabatic connection path*

The potential $\hat{u}_\lambda(r)$ can be a local potential, chosen so that the density remains constant along the adiabatic connection path, $\rho^0 = \rho^\lambda = \rho$, as in the formulation by Langreth and

Perdew [14]. Eqs. (9)-(8) can then be simplified, because

$$\text{tr } \mathbf{u}_0\gamma^0 + \text{tr } \int_0^1 \frac{\partial \mathbf{u}_\lambda}{\partial\lambda}\gamma^\lambda d\lambda = \text{tr } \mathbf{u}_0\rho + \text{tr } (\mathbf{u}_1 - \mathbf{u}_0)\rho = 0 \tag{10}$$

vanishes as $\hat{u}_1 = 0$ to be consistent with the physical Hamiltonian (Eq. (7)). The adiabatic connections Eqs. (9)-(8) then reduce to

$$E^c = \text{tr } \int_0^1 \mathbf{V}(\mathbf{\Gamma}^\lambda - \mathbf{\Gamma}^0)d\lambda \tag{11}$$

and

$$E^c = \text{tr } \int_0^1 \tilde{\mathbf{V}}(\mathbf{G}^\lambda - \mathbf{G}^0)d\lambda. \tag{12}$$

The G-matrix can be derived from the polarization propagator $\mathbf{\Pi}$, which describes density fluctuations,

$$\begin{aligned}\Pi(E)_{ijkl} = &\sum_{n\neq 0} \frac{\langle\Psi_0^N|a_i^\dagger a_j|\Psi_n^N\rangle\langle\Psi_n^N|a_l^\dagger a_k|\Psi_0^N\rangle}{E - \omega_n^N + i\eta} \\ &- \sum_{n\neq 0} \frac{\langle\Psi_0^N|a_i^\dagger a_j|\Psi_n^N\rangle\langle\Psi_n^N|a_l^\dagger a_k|\Psi_0^N\rangle}{E + \omega_n^N - i\eta}\end{aligned}$$

resulting in the well-known ACFD theorem

$$\begin{aligned}E^c &= \text{tr } \int_0^1 \tilde{\mathbf{V}}(\mathbf{G}^\lambda - \mathbf{G}^0)d\lambda \\ &= \frac{-1}{2\pi i}\int_0^1 \int_{-i\infty}^{+i\infty} e^{-E\eta}\text{tr } \tilde{\mathbf{V}}[\mathbf{\Pi}^\lambda(E) - \mathbf{\Pi}^0(E)]dEd\lambda \qquad (13) \\ &= \frac{-1}{2\pi i}\int_0^1 \int_{-i\infty}^{+i\infty} e^{-E\eta}\int d\mathbf{x}d\mathbf{x}'\int \frac{\Pi^\lambda(\mathbf{x},\mathbf{x}',E) - \Pi^0(\mathbf{x},\mathbf{x}',E)}{|\mathbf{r}-\mathbf{r}'|}dEd\lambda. \qquad (14)\end{aligned}$$

This equation has been extensively used in conjunction with the ph-PRA, the lowest-order approximation to the polarization propagator $\mathbf{\Pi}$. The second-order density matrix can be derived from the pp-propagator (3), resulting in an equivalent adiabatic connection for the correlation energy in terms of pairing matrix fluctuations:

$$\begin{aligned}E^c &= \text{tr } \int_0^1 \mathbf{V}(\mathbf{\Gamma}^\lambda - \mathbf{\Gamma}^0)d\lambda \\ &= \frac{-1}{2\pi i}\int_0^1 \int_{-i\infty}^{+i\infty} e^{E\eta}\text{tr } \mathbf{V}[\mathbf{K}^\lambda(E) - \mathbf{K}^0(E)]dEd\lambda \qquad (15) \\ &= \frac{-1}{2\pi i}\int_0^1 \int_{-i\infty}^{+i\infty} e^{E\eta}\int d\mathbf{x}d\mathbf{x}'\frac{K^\lambda(\mathbf{x},\mathbf{x}',E) - K^0(\mathbf{x},\mathbf{x}',E)}{|\mathbf{r}-\mathbf{r}'|}dE. \qquad (16)\end{aligned}$$

This adiabatic connection formulates the correlation energy in terms of dynamic pairing matrix fluctuations and is therefore also a fluctuation-dissipation theorem.

2. Harris-Jones Adiabatic Connection path

The Harris-Jones adiabatic connection provides an alternative to the constant-density AC [36]. The potential $\hat{u}_\lambda$ is local and linear in lambda, $\hat{u}_\lambda = (1-\lambda)\hat{u}_0$, such that $\hat{H}_\lambda = \hat{h} + (1-\lambda)\hat{u}_0 + \lambda\hat{V}$. The density is not constrained except at the end points, $\rho^1 = \rho^0$. The one-electron part in eqs. (8-9) is then

$$\text{tr } \mathbf{u}_0\gamma^0 + \text{tr } \int_0^1 \frac{\partial \mathbf{u}_\lambda}{\partial\lambda}\gamma^\lambda d\lambda = -\text{tr } \int_0^1 \mathbf{u}_0(\rho^\lambda - \rho^0)d\lambda.$$

so that eqs. (8-9) reduce to

$$E^c = \text{tr } \int_0^1 \mathbf{V}(\mathbf{\Gamma}^\lambda - \mathbf{\Gamma}^0)d\lambda - \text{tr } \int_0^1 \mathbf{u}_0(\rho^\lambda - \rho^0)d\lambda \tag{17}$$

$$E^c = \text{tr } \int_0^1 \tilde{\mathbf{V}}(\mathbf{G}^\lambda - \mathbf{G}^0)d\lambda - \sum_{ijk}\int_0^1 \langle ij|ki\rangle(\gamma^\lambda_{jk} - \gamma^0_{jk})d\lambda$$
$$- \text{tr } \int_0^1 \mathbf{u}_0(\rho^\lambda - \rho^0)d\lambda, \tag{18}$$

where the density changes along the adiabatic connection path.

3. Linear Adiabatic Connection path without density constraints

The linear adiabatic connection path $\hat{u}_\lambda = (1-\lambda)\hat{u}_0$ can also be used with a - possibly non-local - potential $\hat{u}_0$ for which $\rho^0 \neq \rho^1$. This makes it possible to establish an adiabatic connection between the interacting system and any uncorrelated reference.

$$E^c = \text{tr } \int_0^1 \mathbf{V}(\mathbf{\Gamma}^\lambda - \mathbf{\Gamma}^0)d\lambda - \text{tr } \int_0^1 \mathbf{u}_0(\gamma^\lambda - \gamma^{0)}d\lambda \tag{19}$$

$$E^c = \text{tr } \int_0^1 \tilde{\mathbf{V}}(\mathbf{G}^\lambda - \mathbf{G}^0)d\lambda - \sum_{ijk}\int_0^1 \langle ij|ki\rangle(\gamma^\lambda_{jk} - \gamma^0_{jk})d\lambda$$
$$- \text{tr } \int_0^1 \mathbf{u}_0(\gamma^\lambda - \gamma^0)d\lambda, \tag{20}$$

In contrast to the constant-density or the Harris-Jones adiabatic connection, which require the exact KS reference potential to satisfy the density constraint $\rho^0 = \rho^1$, this adiabatic connection is valid for any non-interacting reference.

4. Generalized Adiabatic Connection paths

The linear dependence of the Hamiltonian Eq. (7) on the interaction strength can be further generalized: the electron-electron interaction may have a nonlinear dependence on the interaction strength λ [37] as long as the end points 0 and b correspond to the non-interacting reference system and the fully interacting system [37]. Assuming the form $\hat{H} = \hat{h} + \hat{u}_\lambda + \hat{W}_\lambda$, with $\hat{u}_b = 0$, $\hat{W}_0 = 0$ and $\hat{W}_b = \frac{1}{r_{12}}$, the energy can be expressed as

$$\begin{aligned} E - E^0 &= \int_0^b \langle \Psi^\lambda | \frac{\partial \hat{H}_\lambda}{\partial \lambda} | \Psi^\lambda \rangle d\lambda \\ &= \text{tr} \int_0^b \frac{\partial \mathbf{W}_\lambda}{\partial \lambda} \mathbf{\Gamma}^\lambda d\lambda + \text{tr} \int_0^b \frac{\partial \mathbf{u}_\lambda}{\partial \lambda} \gamma^\lambda d\lambda \qquad (21) \\ E - E^{HF}[\gamma^0] &= \text{tr} \int_0^b \frac{\partial \mathbf{W}_\lambda}{\partial \lambda} \mathbf{\Gamma}^\lambda d\lambda - \text{tr}\ \mathbf{V}\mathbf{\Gamma}^0 + \text{tr}\ \mathbf{u}_0 \gamma^0 \\ &\quad + \text{tr} \int_0^b \frac{\partial \mathbf{u}_\lambda}{\partial \lambda} \gamma^\lambda d\lambda \qquad (22) \end{aligned}$$

If the potential $\hat{u}_\lambda$ is local and chosen to keep the density constant along the AC path, similar to Eq. (10),

$$\text{tr} \int_0^b \frac{\partial \mathbf{u}_\lambda}{\partial \lambda} \gamma^\lambda d\lambda = -\text{tr}\ \mathbf{u}_0 \rho^0$$

so eq. (22) simplifies to

$$\begin{aligned} E - E^{HF}[\gamma^0] &= \text{tr} \int_0^b \frac{\partial \mathbf{W}_\lambda}{\partial \lambda} \mathbf{\Gamma}^\lambda d\lambda - \text{tr}\ \mathbf{V}\mathbf{\Gamma}^0 \qquad (23) \\ &= \text{tr} \int_0^b \frac{\partial \mathbf{W}_\lambda}{\partial \lambda} \mathbf{\Gamma}^\lambda d\lambda - \text{tr}\ \mathbf{W}_b \mathbf{\Gamma}^0. \qquad (24) \end{aligned}$$

A suitable choice for the non-linear potential $\hat{W}_\lambda$ is for example the error function, for which the fully interacting system is obtained at $b = 1$

$$\hat{W}_\lambda^{erf}(r_{12}) = \frac{erf\left(\frac{\lambda}{1-\lambda} r_{12}\right)}{r_{12}}$$

and the correlation energy expression (23) becomes

$$E - E^{HF}[\gamma^0] = \text{tr} \int_0^1 \frac{\partial \mathbf{W}_\lambda^{erf}}{\partial \lambda} \mathbf{\Gamma}^\lambda d\lambda - \text{tr}\ \mathbf{V}\mathbf{\Gamma}^0$$

with

$$\frac{\partial \hat{W}_\lambda^{erf}(r_{12})}{\partial \lambda} = \frac{2e^{-\left(\frac{\lambda}{1-\lambda} r_{12}\right)^2}}{\sqrt{\pi}(1-\lambda)^2}.$$

5. *Numerical illustrations on the adiabatic connection in terms of pairing matrix fluctuations*

From a practical point of view, the constant-density adiabatic connection path is most useful as it only requires knowledge of the pp-propagator $\mathbf{K}^\lambda$ along the adiabatic connection path. We will use this form of the adiabatic connection in the numerical illustrations of the lowest-order approximation to the pp-propagator, the particle-particle random phase approximation (pp-RPA) in section IV. We will analyze the pp-RPA energy contribution along the adiabatic connection, given by $U(\lambda)$,

$$\begin{aligned} U(\lambda)^{pp} &= \text{tr } \mathbf{V}(\mathbf{\Gamma}^\lambda - \mathbf{\Gamma}^0) \\ &= \frac{-1}{2\pi i}\int_{-i\infty}^{+i\infty} e^{E\eta}\text{tr } \mathbf{V}[\mathbf{K}^\lambda(E) - \mathbf{K}^0(E)]dE \\ &= \sum_n \sum_{p<q,r<s}^{o+v} (\chi_{rs}^{n,N-2})^* \chi_{pq}^{n,N-2} V_{pqrs} - \sum_{i<j}^{o} V_{ijij}, \end{aligned} \tag{25}$$

such that the area under the graph of $U(\lambda)$ represents the correlation energy, $E^c = \int_0^1 U(\lambda)d\lambda$. In the above equation $\chi_{ij}^{n,N-2} = \langle \Psi_n^{N-2}|a_i a_j|\Psi_0^N\rangle$. For comparison, we will show analogous plots for the ph-RPA correlation energy,

$$\begin{aligned} U(\lambda)^{ph} &= \text{tr } \tilde{\mathbf{V}}(\mathbf{G}^\lambda - \mathbf{G}^0) \\ &= \frac{-1}{2\pi i}\int_{-i\infty}^{+i\infty} e^{-E\eta}\text{tr } \tilde{\mathbf{V}}[\mathbf{\Pi}^\lambda(E) - \mathbf{\Pi}^0(E)]dE \\ &= \sum_n \sum_{ij}^{o} \sum_{ab}^{v} (\chi_{jb}^n)^* \chi_{ia}^n \tilde{V}_{iajb} - \sum_{i}^{o}\sum_{a}^{v} \tilde{V}_{iaia}, \end{aligned} \tag{26}$$

where $\chi_{ia}^n = \langle \Psi_n^N|a_a^\dagger a_i|\Psi_0^N\rangle$. The accurate reference calculations we will compare to are based on the variationally optimized second-order density matrix (v2DM) method under two-positivity conditions[38–40],

$$U(\lambda)^{v2DM} = \text{tr } \mathbf{V}(\mathbf{\Gamma}^\lambda - \mathbf{\Gamma}^0) \tag{27}$$

where the density is assumed to be constant, just like in the pp-RPA and ph-RPA calculation, although this assumption is not generally valid. Unless the density is explicitly constrained along the adiabatic connection path, it changes with the interaction strength, and only expression Eq. (19) is exact in this case. We therefore also present v2DM reference calculations using expression Eq. (19)

$$U(\lambda)^{v2DM*} = \text{tr } \mathbf{V}(\mathbf{\Gamma}^\lambda - \mathbf{\Gamma}^0) - \text{tr } \mathbf{u}_0(\gamma^\lambda - \gamma^0). \tag{28}$$

Since this adiabatic connection makes no assumption on the density along the path and the two-positivity conditions are exact for two-electron systems, Eq. (28) yields exact reference values for two-electron systems and generally very accurate values for three- and four-electron systems. Note that the exact $U(\lambda)$ along this adiabatic connection path is not necessarily convex, unlike $U(\lambda)$ along the constant-density adiabatic connection path. The pp-RPA adiabatic connection path is illustrated and further discussed in figures (1)-(5) of section IV.

C. The particle-particle random phase approximation

The adiabatic connection (16) is in principle exact, but - just like the adiabatic connection in terms of the polarization propagator - it requires an expression for the pp-propagator at each interaction strength. The pp-RPA is the most straightforward approximation to the pp-propagator; it makes the propagator's dependence on the interaction strength explicit. It approximates the interacting propagator $\mathbf{K}$, eq. (3), in terms of the uncorrelated propagator $\mathbf{K}^0$, eq. (4), in the form of a Dyson-like equation, similar in form to the ph-RPA,

$$\mathbf{K}^\lambda(E) = \mathbf{K}^0(E) + \lambda \mathbf{K}^0(E)\mathbf{V}\mathbf{K}^\lambda(E), \tag{29}$$

where all operators are expressed in an anti-symmetrical basis with restricted two-particle indices ij for which $i < j$. Since the non-interacting propagator $\mathbf{K}^0$ only has particle-particle and hole-hole terms the dimension of the matrices $\mathbf{K}^0$ and $\mathbf{K}$ in the pp-RPA is $\frac{o}{2}(o-1) + \frac{v}{2}(v-1)$ where o is the number of holes (occupied orbitals) and v is the number of particles (virtual orbitals). The Dyson-like approximation (29) makes it possible to carry out the lambda-integration in (16) analytically and write the correlation energy in closed form by recognizing that the Dyson-like equation generates an infinite series equivalent to the Taylor expansion for $\ln(\mathbf{I} - \mathbf{K}^0\mathbf{V})$:

$$\begin{aligned}
E^c_{pp} &= \frac{-1}{2\pi i}\int_0^1 \int_{-i\infty}^{+i\infty} \text{tr}\,[\mathbf{K}^\lambda(E)\mathbf{V} - \mathbf{K}^0(E)\mathbf{V}]dEd\lambda \\
&= \frac{-1}{2\pi i}\int_0^1 \int_{-i\infty}^{+i\infty} \sum_{n=2}^{\infty} \lambda^{n-1}\text{tr}\,[(\mathbf{K}^0\mathbf{V})^n]dEd\lambda \\
&= -\frac{1}{2\pi i}\int_{-i\infty}^{+i\infty} \sum_{n=2}^{\infty} \frac{1}{n}\text{tr}\,[(\mathbf{K}^0\mathbf{V})^n]dE \qquad (30) \\
&= \frac{1}{2\pi i}\int_{-i\infty}^{+i\infty} \text{tr}\,[\ln(\mathbf{I} - \mathbf{K}^0\mathbf{V}) + \mathbf{K}^0\mathbf{V}]dE. \qquad (31)
\end{aligned}$$

This is just one way to characterize the pp-RPA correlation energy. The Dyson-like equation can be reformulated as an eigenvalue problem by multiplying each side of the equation by $(E - \omega_n^{N-2})$ and subsequently taking the limit $E \to \omega_n^{N-2}$ to single out the terms that have $(E - \omega_n^{N-2})$ in the denominator on each side of the Dyson-like equation. This reveals a symplectic eigenvalue problem in the eigenvalues ω_n and the eigenvectors χ^n

$$\sum_{c<d} \left(V_{abcd} + \delta_{ac}\delta_{bd}\omega^0_{ab}\right) \chi^n_{cd} + \sum_{h<i} V_{abhi}\chi^n_{hi} = \omega_n \chi^n_{ab}$$
$$\sum_{c<d} V_{hicd}\chi^n_{cd} + \sum_{j<k} \left(V_{hijk} - \delta_{jh}\delta_{ik}\omega^0_{hi}\right) \chi^n_{jk} = -\omega_n \chi^n_{hi},$$

where $\omega^0_{pq} = \epsilon_p + \epsilon_q - 2\nu$. The same set of equations emerges for the double electron addition energies ω_n^{N+2}. These equations can be written in the form $\mathbf{R}\chi = \omega\mathbf{M}\chi$ with $\mathbf{M} = \begin{pmatrix} \mathbf{1} & \mathbf{0} \\ \mathbf{0} & \mathbf{-1} \end{pmatrix}$ or

$$\begin{pmatrix} \mathbf{A} & \mathbf{B} \\ \mathbf{B}^\dagger & \mathbf{C} \end{pmatrix} \begin{pmatrix} \mathbf{X} \\ \mathbf{Y} \end{pmatrix} = \omega \begin{pmatrix} \mathbf{1} & \mathbf{0} \\ \mathbf{0} & \mathbf{-1} \end{pmatrix} \begin{pmatrix} \mathbf{X} \\ \mathbf{Y} \end{pmatrix} \tag{32}$$

when the eigenvectors are divided up into pp-vectors $\mathbf{x}$ and hh-vectors $\mathbf{y}$ and the matrix $\mathbf{R}$ is divided accordingly into submatrices $\mathbf{A}$, $\mathbf{B}$ and $\mathbf{C}$, defined as

$$\begin{aligned} A_{abcd} &= \langle ab \| cd \rangle + \delta_{ac}\delta_{bd}\omega^0_{ab} \\ B_{abij} &= \langle ab \| ij \rangle \\ C_{ijkl} &= \langle ij \| kl \rangle - \delta_{ik}\delta_{jl}\omega^0_{ij}. \end{aligned} \tag{33}$$

The indices a, b are particle indices and i, j are hole indices restricted to $a < b$ and $i < j$, and ν is the chemical potential. While the inclusion of the chemical potential is not strictly necessary, it conveniently shifts the double electron addition energies ω_n^{N+2} to be positive and the double ionization energies ω_n^{N-2} to be negative. Due to the use of an antisymmetrized basis, the dimension of the matrix $\mathbf{A}$ is $N_{pp} \equiv \frac{v}{2}(v-1)$ and the dimension of the matrix $\mathbf{C}$ is $N_{hh} \equiv \frac{o}{2}(o-1)$. The correlation energy (31) can then be written in terms of the eigenvalues ω_n (in a similar fashion to the ph-RPA [17], see [28] for a full derivation),

$$E^c_{pp} = \sum_n^{N_{pp}} \omega_n^{N+2} - \text{tr } \mathbf{A} = -\sum_n^{N_{hh}} \omega_n^{N-2} - \text{tr } \mathbf{C}. \tag{34}$$

The symplectic eigenvalue problem (32) can also be derived from the equations of motion (EOM) for the $N + 2$ (or $N - 2$) electron excited states generated by the operators

$\hat{O}^n = \sum_{ab} X^n_{ab} a^\dagger_b a^\dagger_a - \sum_{ij} Y^n_{ij} a^\dagger_j a^\dagger_i$ (or their Hermitian conjugate)[29]. From the Schrödinger equation, an exact double electron addition operator $\hat{O}^n = |\Psi^{N+2}_n\rangle\langle\Psi^N_0|$ must satisfy $[\hat{A},[\hat{H},\hat{O}^n]] = (E^{N+2}_n - E^N_0)[\hat{A},\hat{O}^n]$ for any operator $\hat{A}$. Projecting onto an uncorrelated reference wavefunction, this leads to

$$\langle\Phi^N_0|[a_p a_q,[\hat{H},\hat{O}^n]]|\Phi^N_0\rangle = \omega_n \langle\Phi^N_0|[a_p a_q,\hat{O}^n]|\Phi^N_0\rangle \tag{35}$$

which is completely equivalent to Eq. (32), as the elements $\langle\Phi^N_0|[a_p a_q,[\hat{H},a^\dagger_s a^\dagger_r]]|\Phi^N_0\rangle$ in $\langle\Phi^N_0|[a_p a_q,[\hat{H},\hat{O}^n]]|\Phi^N_0\rangle$ reduce to elements of the pp-RPA matrix $\mathbf{R}$ and the commutators $\langle\Phi^N_0|[a_p a_q,a^\dagger_s a^\dagger_r]|\Phi^N_0\rangle$ in $\langle\Phi^N_0|[a_p a_q,\hat{O}^n]|\Phi^N_0\rangle$ are either zero or one depending on the pp- or hh-nature of the indices pq and rs :

$$\begin{aligned}\langle\Phi^N_0|[a_p a_q,[\hat{H},a^\dagger_s a^\dagger_r]]|\Phi^N_0\rangle &= R_{pqrs}\\ \langle\Phi^N_0|[a_p a_q,a^\dagger_s a^\dagger_r]|\Phi^N_0\rangle &= M_{pqrs}.\end{aligned}$$

The pp-RPA energy can alternatively be interpreted as the sum of all ladder diagrams: every term of the infinite series in Eq. (30) corresponds to a ladder diagram of increasing order. As the summation of all ladder diagrams, the pp-RPA is equivalent to the CCD restricted to ladder diagrams [10, 30, 32]

$$E^c_{pp} = \text{tr}\,[\mathbf{TB}]$$

where the CCD amplitude matrix $\mathbf{T}$ is a solution to the Riccati equation

$$\mathbf{T}^\dagger\mathbf{A} + \mathbf{T}^\dagger\mathbf{B}\mathbf{T}^\dagger + \mathbf{B}^\dagger + \mathbf{C}\mathbf{T}^\dagger = 0. \tag{36}$$

The matrices $\mathbf{A}$, $\mathbf{B}$ and $\mathbf{C}$ are equivalent to those in the symplectic eigenvalue equation (32). This equation can be easily obtained from the eigenvalue equation (32) by identifying $\mathbf{T} = (\mathbf{Y}\mathbf{X}^{-1})^\dagger$ [31, 32]. Since the ladder diagrams summed to obtain the correlation energy are all connected diagrams, the pp-RPA is size-extensive [35].

D. Stability of the particle-particle random phase approximation

The pp-RPA does not suffer from instabilities like the ph-RPAX, i.e. the ph-RPA with exchange in the two-electron integrals. The ph-RPA is almost exclusively used in its 'direct' formulation, which neglects the exchange terms in the two-electron integrals, within

the DFT community. This preference is motivated by the inherent instability of the ph-RPAX, but neglecting exchange terms also makes it easier to reduce its computational cost via resolution-of-the-identity or density-fitting techniques. Even though the pp-RPA fully accounts for the anti-symmetry of the pp-propagator, it does not suffer from such instabilities. In contrast to the ph-RPAX matrix, which determines the stability of the reference wavefunction under orbital rotations and therefore often breaks down in cases with near-degeneracies, the pp-PRA matrix determines the stability of the reference wavefunction under double ionization or electron addition.

The energies for a physical system at integer electron number decrease monotonically in a convex manner,

$$E_0^{N+2} - E_0^{N+1} \geq E_0^{N+1} - E_0^N \geq E_0^N - E_0^{N-1} \geq E_0^{N-1} - E_0^{N-2} \tag{37}$$

This means that the system is stable with respect to the propornation reaction from two $N-$electron systems to an $N+2$ and an $N-2$ electron system. Since the chemical potential can be defined as either the left- or right-derivative of the energy with respect to electron number,

$$\nu^+ = E_0^{N+1} - E_0^N$$
$$\nu^- = E_0^N - E_0^{N-1}$$

the inequalities (37) can be written as

$$E_0^{N+2} - E_0^N - 2\nu^+ \geq 0$$
$$E_0^N - E_0^{N-2} - 2\nu^- \leq 0$$

so the double electron addition and removal energies defined before are positive and negative, respectively,

$$\omega_n^{N+2} = E_n^{N+2} - E_0^N - 2\nu \geq 0$$
$$\omega_n^{N-2} = E_0^N - E_n^{N-2} - 2\nu \leq 0.$$

where the chemical potential $\nu \in [\nu^+, \nu^-]$. This physical requirement on the wavefunction

implies that the pp-RPA matrix is positive-semidefinite. For any $c = \sum_n a_n \chi^i$

$$
\begin{aligned}
&\sum_{ijkl} c^*_{kl} \langle \Phi_0^N | [a_k a_l, [H, a_j^\dagger a_i^\dagger]] | \Phi_0^N \rangle c_{ij} \\
&= \mathbf{c}^\dagger \mathbf{R} \mathbf{c} \\
&= \sum_{mn}^{N_{pp}+N_{hh}} a_n^* (\chi^n)^\dagger \mathbf{R} \chi^m a_m \\
&= \sum_{mn}^{N_{pp}+N_{hh}} \omega_m a_n^* (\chi^n)^\dagger \mathbf{M} \chi^m a_m \\
&= \sum_{n}^{N_{pp}+N_{hh}} \omega_m |a_n|^2 (\chi^n)^\dagger \mathbf{M} \chi^n \\
&= \sum_{n}^{N_{pp}} \omega_n^{N+2} |a_n|^2 |(\chi^n)^\dagger \mathbf{M} \chi^n| + \sum_{n}^{N_{hh}} (-\omega_n^{N-2}) |a_n|^2 |(\chi^n)^\dagger \mathbf{M} \chi^n| \\
&\geq 0
\end{aligned}
$$

Here we have used the ortogonality of the eigenvectors, $(\chi^n)^\dagger \mathbf{M} \chi^m = 0$ for $m \neq n$ and the normalization of the eigenvectors: eigenvectors dominated by pp-elements involve the $N+2$-electron states, have a positive norm $(\chi^n)^\dagger \mathbf{M} \chi^n > 0$ and can thus be normalized to 1, whereas eigenvalues dominated by hh-elements involve the $N-2$-electron states, have a negative norm $(\chi^n)^\dagger \mathbf{M} \chi^n < 0$ and can thus be normalized to -1. So the stability of the state under double ionization and electron addition implies that the pp-RPA matrix is positive semi-definite. Conversely, positive-semidefiniteness of the pp-RPA matrix guarantees that the symplectic eigenvalue problem produces N_{pp} real positive double electron addition energies and N_{hh} real negative double ionization energies[50] and therefore assures that the correlation energy Eq. (34) is real.

The Hartree-Fock ground state for systems described by repulsive Coulombic interactions must satisfy the stability requirement. From the EOM perspective, Eq. (35), it is clear that the elements of the pp-RPA matrix (32) are the elements of the double commutator matrix $R_{klij} = \langle \Phi_0^N | [a_k a_l, [H, a_j^\dagger a_i^\dagger]] | \Phi_0^N \rangle$ which determines the second derivative of the energy with respect to double ionization or electron removal. Suppose $e^{i\hat{u}} | \Phi_0^N \rangle$, with $\hat{u}$ a double ionization/electron addition operator $\hat{u} = \frac{1}{2} \sum_{ij} u_{ij} a_j^\dagger a_i^\dagger + u_{ij}^* a_i a_j$, represents a small transformation of the uncorrelated wavefunction Φ_0^N that breaks the particle number symmetry, since $\hat{u}$ does not commute with the electron number operator $\hat{N}$. The second-order derivative

of the energy under such a transformation, evaluated at Ψ_0^N is

$$\begin{aligned}\frac{\partial^2 E}{\partial u_{kl}^* \partial u_{ij}}\Big|_{\hat{u}=0} &= \frac{\partial^2}{\partial u_{kl}^* \partial u_{ij}} \langle \Phi_0^N | e^{-i\hat{u}} \hat{H} e^{i\hat{u}} | \Phi_0^N \rangle \Big|_{\hat{u}=0} \\ &= \langle \Phi_0^N | [a_k a_l, [\hat{H}, a_j^\dagger a_i^\dagger]] | \Phi_0^N \rangle.\end{aligned}$$

If the double commutator matrix $\mathbf{R}$ is not positive-semidefinite, the eigenvectors with negative eigenvalue indicate that there exists a Bogoliubov transformation to a superfluid state with $\langle \hat{N} \rangle^2 \neq \langle \hat{N}^2 \rangle$ and non-vanishing pairing matrix with lower energy. This is impossible: the energy contribution from the non-zero pairing matrix in such a state is of the form $\sum_{p<q,r<s} \kappa_{pq}^* V_{pqrs} \kappa_{rs}$ [17] and is manifestly positive for a repulsive interaction $\hat{V}$. The pp-RPA based on a HF reference must therefore have real eigenvalues and correlation energies.

III. COMPUTATIONAL DETAILS

The numerical illustrations on the pp-RPA in section IV are post-Hartree-Fock (HF) or post-Kohn-Sham (KS) calculations based on HF or KS reference wavefunctions from Gaussian03 [41] for the dissociation graphs and HF or KS reference wavefunctions from QM4D [42] for the weakly bound dimers. For the subsequent pp-RPA calculations, we used our own implementation. For the discussion of the molecular dissociation graphs and the adiabatic connection, we used the local density approximation (LDA) reference, while for the weakly bonded dimers we used HF references to enable comparison to second-order Möller-Plesset perturbation theory (MP2). For the accurate reference calculations along the adiabatic connection path we used our own semi-definite optimization algorithm to optimize the second-order density matrix under two-positivity conditions [38]. We denote this method as 'v2DM'.

We used a cc-pVDZ basis set for the calculations of the dissociation graphs and adiabatic connection graphs, a cartesian d-aug-cc-pVTZ basis sets for the Ar dimer and aug-cc-pVDZ for the other van der Waals systems, both limited to f-angular momentum functions.

IV. NUMERICAL ILLUSTRATIONS ON THE PP-RPA

The adiabatic connection (31) provides a framework for developing density functionals based on pairing matrix fluctuations. The most straightforward functional is perhaps

the pp-RPA, the lowest order approximation to the pp-propagator, which may serve as an illustration of this new path for developing density functionals. We therefore examine the pp-RPA in this section with applications to molecular dissociation and thermodynamic properties. We focus in particular on its comparison to the ph-RPA, since the two RPA's can be viewed as representatives of the two different adiabatic connection perspectives for the exact exchange-correlation energy, Eq. (14) and (16).

The pp-RPA gives the correct dissociation limit for the two paradigmatic cases for strong static correlation and delocalization, H_2 and H_2^+ [28]. The most commonly used functionals today, local density approximations, generalized gradient approximations and hybrid density functional approximations, fail to describe both dissociation limits well within a restricted framework. The success of these DFA's for many applications relies on error cancellations between the exchange and correlation part of the functionals, so they fail to describe the extremes of the spectrum, where either correlation or exchange dominate. The H_2 and H_2^+ molecules are paradigmatic examples of these extremes: describing the dissociated H_2 correctly requires strong left-right static correlation, which DFA's typically underestimate, while describing the dissociated H_2^+ requires exact exchange but no correlation, so even hybrid functionals that mix in a fraction of exact exchange fail to describe the two extremes. The pp-RPA produces the correct dissociation limit for both H_2 and H_2^+, while the ph-RPA fails to bind the H_2^+ ion [28]. At shorter bond lengths, near 10 Å, the pp-RPA energy for H_2 shows an unphysical repulsion, which is also present in the ph-RPA energy, albeit to lesser extent. This unphysical barrier for dissociation occurs for different references and its origin in the ph-RPA has been the object of speculation, with some authors attributing it to the lack of self-consistency[43][44] – although this hypothesis has recently been rejected by actual self-consistent implementations[45] – and others attributing it to the lack of higher order excitations in the ph-RPA [26]. Unlike the ph-RPA, the pp-RPA is self-interaction free: it reduces to the HF functional for one-electron systems. So it has no delocalization error for the dissociated H_2^+ molecule and produces equally good potential energy functions for less trivial odd-electron systems [28]. The ph-RPA has large self-interaction errors for these systems; it adds such a large correlation energy to the exact exchange that the H_2^+ and He_2^+ molecules are not bound.

The adiabatic connection provides an additional perspective on the pp-RPA energy contribution as a function of the interaction strength. Figs. 1, 2 and 3 illustrate the correlation

energy contribution in the pp-RPA along the adiabatic connection path for H_2. In the dissociation limit, the pp-RPA energy along the constant-density AC path approaches the step function, much like the exact connection. Near equilibrium, the pp-RPA energy along the constant-density AC path has the exact initial slope but falls short in the interacting limit and therefore slightly underestimates the correlation energy. Such an energy profile along the adiabatic connection path seems to be typical in molecules near equilibrium geometry. Near 10 Å the pp-RPA and the ph-RPA severely underestimate the correlation energy, resulting in the unphysical barrier in the dissociation of H_2. Figs. (4) and (5) illustrate how the pp-RPA has no self-interaction error in H_2^+ or He_2^+ while the ph-RPA gives a much too large correlation energy at any interaction strength.

The restricted dissociation of the N_2 molecule proves an even greater challenge than the dissociation of H_2 because it involves a simultaneous stretch of three bonds. The ph-RPA prevails for such cases, as it has no static correlation error for the stretched N_2 molecule, while the pp-RPA energy is much too low, similar to truncated coupled cluster methods like CCSD [28]. The failure of the pp-RPA for such cases, however, seems to have little adverse effects on thermodynamic properties – even the reaction energies surveyed in previous work are rather good[46] – perhaps because chemical reactions rarely involve simultaneous multiple bond breaking.

One of the main reasons for the renewed interest in the ph-RPA has been its ability to capture long-range interactions in a seamless manner with the correct R^{-6} asymptotic decay [7, 23–25]. It has served as a source of inspiration for more empirical density functionals. Can the pp-RPA also describe this type of interactions? Perhaps surprisingly, the pp-RPA gives very good interaction energies for several types of non-bonded interactions, competitive with or even better than the ph-RPA energies [46]: the pp-RPA(PBE) has an overall MSE and MUE of -0.28 and 0.60 kcal/mol while the ph-RPA(PBE) has an MSE and MUE of 1.86 and 1.86 kcal/mol. A possible explanation for these good results is the correct second-order energy term in the pp-RPA: the second-order term in eq. (30) is exact, equivalent to MP2 correlation energy. The ph-RPA has a similar second-order energy term but neglects the exchange terms. Since the second-order energy term is the predominant term in describing weak interactions, this may explain why the pp-RPA gives surprisingly good non-bonded interaction energies. Figure (6) supports this explanation: upon dissociation, the pp-RPA interaction energy for the weakly interacting noble gas dimer Ar_2 nearly equals the MP2 in-

teraction energy, although MP2 binds the Ar dimer more strongly (fig. 7). Its correct second order energy term also ensures a physically correct R^{-6} asymptotic decay of the interaction energy, as illustrated in figure (6). Calculations on the van der Waals database explored in previous work [46] also demonstrate that the second-order energy term constitutes the main part of the interaction energy (figure 8).

The pp-RPA gives much better atomization energies than the ph-RPA and describes reaction barriers with similar accuracy. While the adiabatic connection graphs (figures 1-5) suggest that the pp-RPA tends to underestimate the correlation energy in the interacting limit, it gives much better atomization energies - which rely on relative, rather than absolute, energies - than the ph-RPA. The current literature on ph-RPA molecular atomization energies mostly focuses on small molecules [12, 47, 48]. The mean signed error in the ph-RPA atomization energies for such few-atomic systems is on the order of +10 kcal/mol. This phenomenon of underbinding in the ph-RPA is well-known [12, 47]. The ph-RPA typically overestimates correlation energies, but it over-correlates atoms more strongly than molecules, such that it underestimates atomization energies. For bigger molecules, this problem becomes even more pronounced: the error in the ph-PRA atomization energies continues to grow with the number of atoms in the molecule, which is reflected in its mean signed error of 22.7 kcal/mol for the whole G2 set, equal to its mean unsigned error. The pp-RPA does not suffer from this problem: its mean signed error for the whole G2 set is a mere -1.9 kcal/mol and its mean unsigned error is 8.3 kcal/mol, much lower than that for the ph-RPA [46]. The pp-RPA and ph-RPA give rather similar reaction energies. For reaction barriers involving the molecules contained in the G2 set, the pp-RPA and ph-RPA errors are 2.4 and 2.3 kcal/mol respectively, and for the DBH24 reaction enthalpy set their respective errors are 3.2 and 2.5 kcal/mol. So while the pp-RPA generally seems to underestimate absolute correlation energies, it describes thermodynamic properties well.

The computational cost of the pp-RPA scales as $O(o^2v^4)$ without making further approximations. While the full diagonalization of the pp-RPA matrix, eq. (33), may seem to require $O(v^6)$ operations, not all of the eigenvalues are are needed to compute the correlation energy $E^c = -\sum_n \omega_n^{N-2} - \mathrm{tr}\ \mathbf{C}$; the $O(o^2)$ double ionization energies suffice. The lowest required computational cost is then $O(o^2v^4)$. This agrees with the cost of the equivalent ladder-CCD formulation, eq. (36): the term that dominates the floating point operation count for the ladder-CCD formulation of the pp-RPA is the same $O(o^2v^4)$ term that dominates the

operation count for CCSD [49].

V. CONCLUSIONS

We have formulated an adiabatic connection for the correlation energy in terms of pairing matrix fluctuations. This adiabatic connection formalism is in principle exact, but requires an expression for the pp-propagator at each interaction strength. It thus lays the theoretical foundations for approximate density functionals based on pairing matrix fluctuations. The pp-RPA is the lowest-order approximation to the pp-propagator. Judging from the numerical illustrations on the pp-RPA, the adiabatic connection eq. (16) may lead to interesting new functionals: the pp-RPA captures the strong static correlation in the dissociation limit of H2 and other single bond systems, has no delocalization error and is self-interaction free. Despite its tendency to underestimate correlation energies, the pp-RPA gives good relative energies and thermodynamic data – in fact, it gives much better atomization energies than the ph-RPA because it does not systematically underbind like the ph-RPA. Its exact second-order energy ensures a correct description of non-bonded interactions. It is size-extensive. Nonetheless, it fails for the simultaneous multiple bond-breaking in N_2, and even though common chemical reactions rarely involve simultaneous multiple bond breaking, this is an undesirable feature that can perhaps be alleviated in further development of DFA's derived from the pp-RPA or the pp-propagator.

The adiabatic connection allows for a wealth of approximate density functionals based on pairing matrix fluctuations and their computational scaling obviously depends on the nature of the functional. The pp-RPA is, with its $O(o^2v^4)$ operation count, computationally expensive, especially due to its high dependence on the virtual orbitals. Because of the explicit antisymmetry of the pp-propagator its computational cost is not as straightforwardly reduced by resolution-of-the-identity techniques as the ph-RPA, which neglects the exchange terms in the two-electron integrals. We are currently exploring other approaches to reduce its computational cost. The adiabatic connection framework opens the way for further approximations to obtain density functionals based on pairing matrix fluctuations with low computational scaling.

Figure 1: In H_2 near equilibrium, the pp-RPA slightly underestimates the correlation energy, given by the area under the curve of $U(\lambda)$ along the constant-density path, Eq. (25). The v2DM$*$ curve shows the exact correlation energy, obtained by the adiabatic connection of Eq. (28), while the v2DM curve assumes a constant-density along the path as an approximation, Eq. (27).

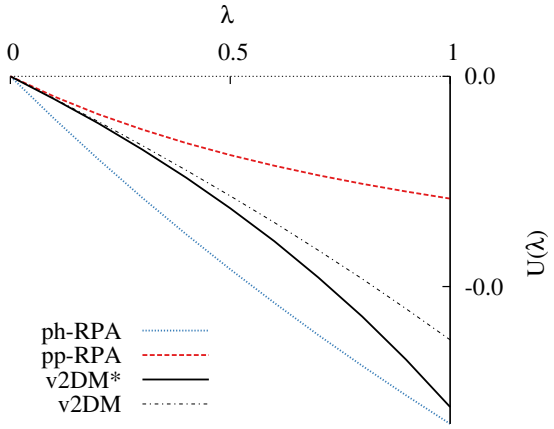

Figure 2: In H_2 at 10 Å the pp-RPA and the ph-RPA significantly underestimate the correlation energy, given by the area under their respective curves, leading to the unphysical barrier in the dissociation graph for H_2. The area under the v2DM* curve shows the exact correlation energy and the v2DM curve shows an approximate constant-density path.

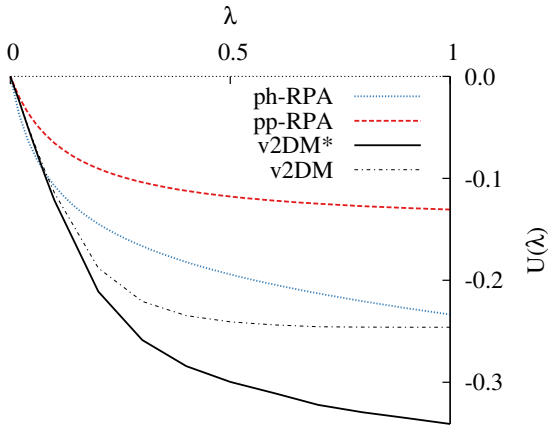

Acknowledgments

Support from FWO-Flanders (Scientific Research Fund Flanders) (H.v.A), the Office of Naval Research (N00014-09- 0576) and the National Science Foundation (CHE-09-11119) (W.Y.) is appreciated.

Figure 3: For two H atoms separated by 10000 Å the pp-RPA and the ph-RPA correctly reproduce the strong static correlation energy, given by the area under their respective curves. The area under the v2DM* curve shows the exact correlation energy and the v2DM curve shows an approximate constant-density path.

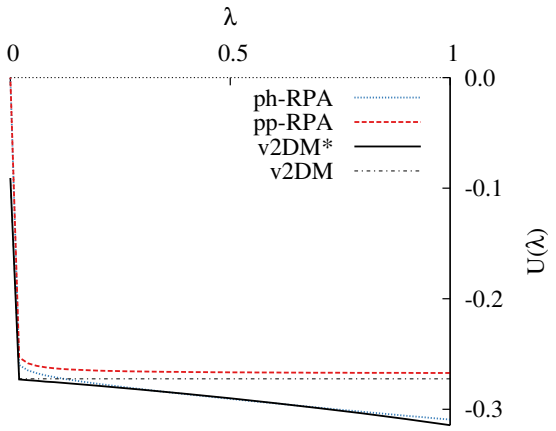

Figure 4: The pp-RPA correctly adds no correlation energy to the exact exchange in H_2^+ at 10 Å and is thus self-interaction free, while the ph-RPA has a large self-interaction error, given by the area under its curve.

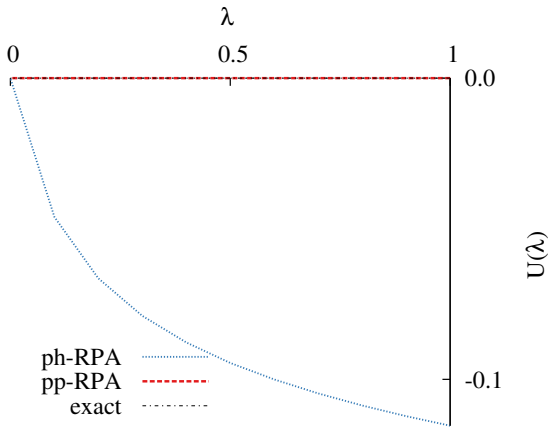

Figure 5: The pp-RPA correctly produces a small correlation energy for He_2^+ at 10 Å, given by the area under the curve, while the ph-RPA adds such a large correlation energy to the exact exchange that it fails to bind He_2^+. The area under the v2DM* curve shows the exact correlation energy and the v2DM curve shows an approximate constant-density path.

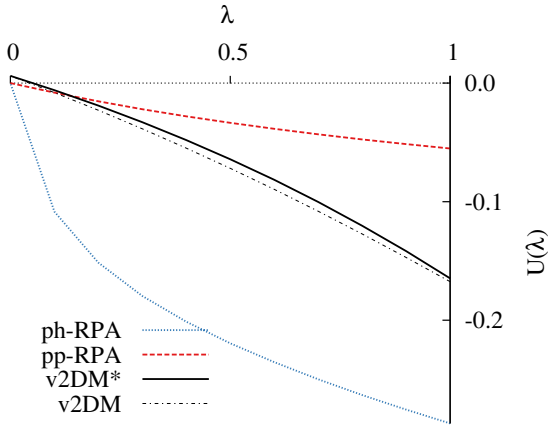

Figure 6: The pp-RPA interaction energy for the Ar dimer has an R^{-6} decay, very similar to the second order energy in MP2, plotted here on a log-log scale alongside an illustrative R^{-6} function.

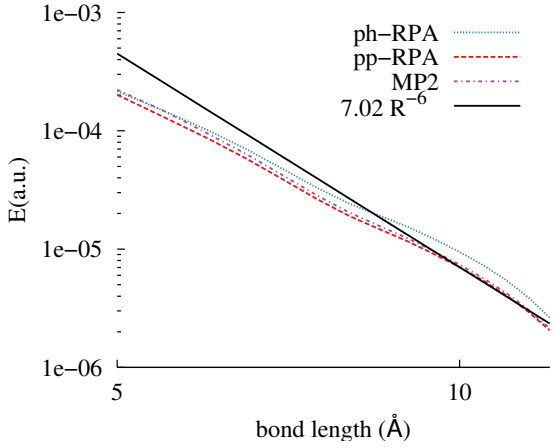

Figure 7: The pp-RPA and the ph-RPA describe the van der Waals interactions in the Ar dimer well. MP2 binds the dimer more strongly.

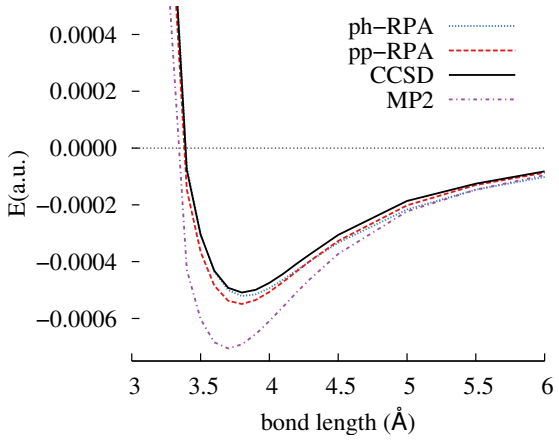

Figure 8: The (counter-poise corrected) pp-RPA interaction energies (in kcal/mol) are very similar to the MP2 interaction energies for a set of van de Waals bonded molecules.

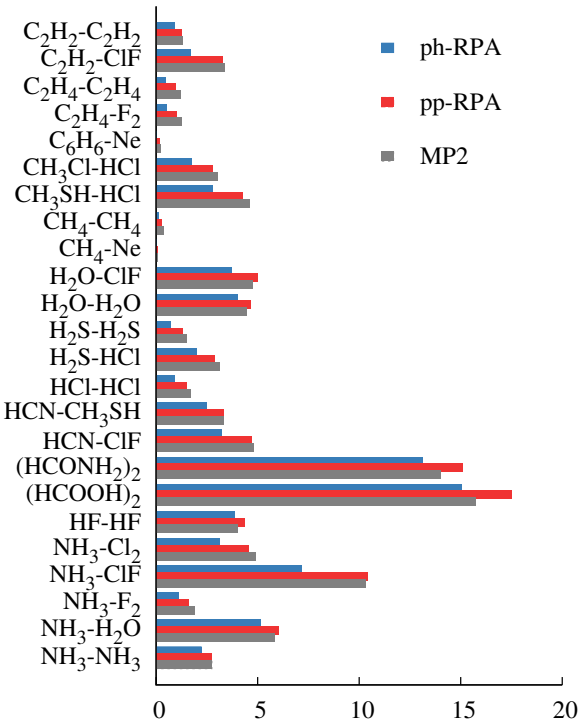

[1] A. J. Cohen, P. Mori-Sanchez, and W. T. Yang. Challenges for density functional theory. *Chem Rev*, 112(1):289–320, 2012.

[2] A. J. Cohen, P. Mori-Sanchez, and W. T. Yang. Fractional charge perspective on the band gap in density-functional theory. *Physical Review B*, 77(11):115123, 2008.

[3] A. Savin. Is size-consistency possible with density functional approximations? *Chemical Physics*, 356(1-3):91–97, 2009.

[4] J. P. Perdew, R. G. Parr, M. Levy, and J. L. Balduz. Density-functional theory for fractional particle number - derivative discontinuities of the energy. *Phys Rev Lett*, 49(23):1691–1694, 1982.

[5] P. Mori-Sanchez, A. J. Cohen, and W. T. Yang. Discontinuous nature of the exchange-correlation functional in strongly correlated systems. *Phys Rev Lett*, 102(6):066403, 2009.

[6] A. J. Cohen, P. Mori-Sanchez, and W. Yang. Insights into current limitations of density functional theory. *Science*, 321(5890):792–4, 2008.

[7] John F. Dobson and Jun Wang. Successful test of a seamless van der waals density functional. *Phys. Rev. Lett.*, 82:2123–2126, 1999.

[8] Manfred Lein, E. K. U. Gross, and John P. Perdew. Electron correlation energies from scaled exchange-correlation kernels: Importance of spatial versus temporal nonlocality. *Phys. Rev. B*, 61:13431–13437, 2000.

[9] Paul A. Johnson, Paul W. Ayers, Peter A. Limacher, Stijn De Baerdemacker, Dimitri Van Neck, and Patrick Bultinck. A size-consistent approach to strongly correlated systems using a generalized antisymmetrized product of nonorthogonal geminals. *Computational and Theoretical Chemistry*, 1003:101, 2013.

[10] Carlos A. Jimenez-Hoyos, Thomas M. Henderson, Takashi Tsuchimochi, and Gustavo E. Scuseria. Projected hartree–fock theory. *The Journal of Chemical Physics*, 136(16):164109, 2012.

[11] K. Burke. Perspective on density functional theory. *Journal of Chemical Physics*, 136(15):150901, 2012.

[12] F. Furche. Molecular tests of the random phase approximation to the exchange-correlation energy functional. *Physical Review B*, 64(19):195120, 2001.

[13] David Bohm and David Pines. A collective description of electron interactions. i. magnetic

interactions. *Phys. Rev.*, 82:625–634, 1951.

[14] D.C. Langreth and J.P. Perdew. The exchange-correlation energy of a metallic surface. *Solid State Communications*, 17(11):1425 – 1429, 1975.

[15] O. Gunnarsson and B. I. Lundqvist. Exchange and correlation in atoms, molecules, and solids by the spin-density-functional formalism. *Phys. Rev. B*, 13:4274–4298, 1976.

[16] Herbert B. Callen and Theodore A. Welton. Irreversibility and generalized noise. *Phys. Rev.*, 83:34–40, 1951.

[17] J. P. Blaizot and G. Ripka. *Quantum Theory of Finite Systems*. MIT Press, 1986.

[18] G. Scuseria, M. Levy, and K. Burke. Special issue in honor of john p. perdew for his 65th birthday. *J Chem Theory Comput*, 5(4):675–678, 2009.

[19] X. G. Ren, P. Rinke, V. Blum, J. Wieferink, A. Tkatchenko, A. Sanfilippo, K. Reuter, and M. Scheffler. Resolution-of-identity approach to hartree-fock, hybrid density functionals, rpa, mp2 and gw with numeric atom-centered orbital basis functions. *New Journal of Physics*, 14(4):043002, 2012.

[20] H. Eshuis, J. Yarkony, and F. Furche. Fast computation of molecular random phase approximation correlation energies using resolution of the identity and imaginary frequency integration. *J Chem Phys*, 132(23):234114, 2010.

[21] J. E. Moussa. Cubic-scaling algorithm and self-consistent field for the random-phase approximation with second-order screened exchange. *ArXiv*, arXiv:1303.3847, 2013.

[22] Daniel Neuhauser, Eran Rabani, and Roi Baer. Expeditious stochastic calculation of random-phase approximation energies for thousands of electrons in three dimensions. *The Journal of Physical Chemistry Letters*, 4(7):1172–1176, 2013.

[23] H. Eshuis and F. Furche. A parameter-free density functional that works for noncovalent interactions. *Journal of Physical Chemistry Letters*, 2(9):983–989, 5 2011.

[24] H. Eshuis and F. U. Furche. Fast implementation of random-phase approximation for molecular correlation energies: Application to weakly interacting systems. *Abstracts of Papers of the American Chemical Society*, 241, 2011.

[25] J. Toulouse, W. M. Zhu, A. Savin, G. Jansen, and J. G. Angyan. Closed-shell ring coupled cluster doubles theory with range separation applied on weak intermolecular interactions. *Journal of Chemical Physics*, 135(8):084119, 2011.

[26] M. Fuchs, Y. M. Niquet, X. Gonze, and K. Burke. Describing static correlation in bond disso-

ciation by kohn-sham density functional theory. *Journal of Chemical Physics*, 122(9):094116, 2005.

[27] P. Mori-Sanchez, A. J. Cohen, and W. T. Yang. Failure of the random-phase-approximation correlation energy. *Physical Review A*, 85(4):042507, 2012.

[28] Helen van Aggelen, Yang Yang, and Weitao Yang. Exchange-correlation energy from pairing matrix fluctuation and the particle-particle random-phase approximation. *Phys. Rev. A*, 88:030501, 2013.

[29] P. Ring and P. Schuck. *The Nuclear Many-Body Problem*. Texts and Monographs in Physics. Springer-Verlag, 1980.

[30] D. L. Freeman. Coupled-cluster summation of the particle-particle ladder diagrams for the two-dimensional electron gas. *J. Phys. C*, 16:711, 1983.

[31] Gustavo E. Scuseria, Thomas M. Henderson, and Ireneusz W. Bulik. Particle-particle and quasiparticle random phase approximations: Connections to coupled cluster theory. *The Journal of Chemical Physics*, 139(10):104113, 2013.

[32] Degao Peng, Stephan N. Steinmann, Helen van Aggelen, and Weitao Yang. Equivalence of particle-particle random phase approximation correlation energy and ladder-coupled-cluster doubles. *The Journal of Chemical Physics*, 139(10):104112, 2013.

[33] Christoph-Maria Liegener. Auger spectra by the green's function method. *Chemical Physics Letters*, 90(3):188 – 192, 1982.

[34] J. V. Ortiz. Qualitative propagator theory of ax[sub 4] auger spectra. *The Journal of Chemical Physics*, 81(12):5873–5888, 1984.

[35] W.H. Dickhoff and D. Van Neck. *Many-body Theory Exposed!: Propagator Description of Quantum Mechanics in Many-body Systems*. World Scientific, 2005.

[36] J Harris and R O Jones. The surface energy of a bounded electron gas. *Journal of Physics F: Metal Physics*, 4(8):1170, 1974.

[37] W. T. Yang. Generalized adiabatic connection in density functional theory. *Journal of Chemical Physics*, 109(23):10107–10110, 1998.

[38] B. Verstichel, H. van Aggelen, D. Van Neck, P. W. Ayers, and P. Bultinck. Variational determination of the second-order density matrix for the isoelectronic series of beryllium, neon, and silicon. *Physical Review A*, 80(3):032508, 2009.

[39] D. A. Mazziotti. Variational minimization of atomic and molecular ground-state energies via

the two-particle reduced density matrix. *Physical Review A*, 65(6): 062511, 2002.

[40] M. Nakata, H. Nakatsuji, M. Ehara, M. Fukuda, K. Nakata, and K. Fujisawa. Variational calculations of fermion second-order reduced density matrices by semidefinite programming algorithm. *Journal of Chemical Physics*, 114(19):8282–8292, 2001.

[41] M. J. Frisch, G. W. Trucks, H. B. Schlegel, G. E. Scuseria, M. A. Robb, J. R. Cheeseman, J. A. Montgomery, Jr., T. Vreven, K. N. Kudin, J. C. Burant, J. M. Millam, S. S. Iyengar, J. Tomasi, V. Barone, B. Mennucci, M. Cossi, G. Scalmani, N. Rega, and G. A. et al. Petersson. Gaussian 03, revision b.05. Gaussian Inc., 2004.

[42] Qm4d, a program for qm/mm simulations.

[43] Thomas M. Henderson and Gustavo E. Scuseria. The connection between self-interaction and static correlation: a random phase approximation perspective. *Molecular Physics*, 108(19-20):2511–2517, 2010.

[44] Andreas Heßelmann and Andreas Görling. Correct description of the bond dissociation limit without breaking spin symmetry by a random-phase-approximation correlation functional. *Phys. Rev. Lett.*, 106:093001, 2011.

[45] Maria Hellgren, Daniel R. Rohr, and E. K. U. Gross. Correlation potentials for molecular bond dissociation within the self-consistent random phase approximation. *The Journal of Chemical Physics*, 136(3):034106, 2012.

[46] Yang Yang, Helen van Aggelen, and Weitao Yang. Benchmark tests and spin adaptation for the particle-particle random phase approximation. *J. Chem. Phys.*, 139(17):174110, 2013.

[47] X. Ren, P. Rinke, C. Joas, and M. Scheffler. Random-phase approximation and its applications in computational chemistry and materials science. *Journal of Materials Science*, 47(21):7447–7471, 2012.

[48] H. Eshuis and F. Furche. Basis set convergence of molecular correlation energy differences within the random phase approximation. *J Chem Phys*, 136(8):084105, 2012.

[49] Timothy J. Lee and Julia E. Rice. An efficient closed-shell singles and doubles coupled-cluster method. *Chem. Phys. Lett.*, 150:406–415, 2013.

[50] It can be proven that the eigenvalue problem $\mathbf{Rx} = \omega\mathbf{Mx}$ has real eigenvalues and eigenvectors when $\mathbf{R}$ is positive-semidefinite.